STABILITY AND SYMMETRY BREAKING IN METAL NANOWIRES

Charles A. Stafford
Department of Physics, University of Arizona
1118 East 4th Street, Tucson, AZ 85721

Abstract A linear stability analysis of metal nanowires is performed in the free-electron model using quantum chaos techniques. It is found that the classical instability of a long wire under surface tension can be completely suppressed by electronic shell effects, leading to stable cylindrical configurations whose electrical conductance is a magic number 1, 3, 5, 6,... times the quantum of conductance.

1. Introduction

I had the good fortune to share an office with Deng Feng Wang when we were graduate students at Princeton, and to share the shores of Lac Léman in Switzerland with him as a postdoc some years later. I always enjoyed Wang's wry sense of humor. Like many of his American friends, he did not think me capable of pronouncing "Deng Feng," insisting that I simply call him "Wang," so that is how I knew him. Wang was always concerned with the happiness of his physics friends, not only scientifically, but also in their personal lives. After many years, I finally succumbed to his exhortations to "get yourself a woman," convincing my girlfriend Helen to move to Tucson with me from Germany, when my academic career brought me back to America.

My career has been inextricably tied to that of Deng Feng Wang. As graduate students, we both studied integrable models of one-dimensional many-body systems. My first foray into the field of metallic nanostructures, which has since become the mainstay of my research program, was in collaboration with Wang. We investigated how interactions between electrons in a metallic ring influence the occupation of the conducting subbands of the ring. We found that repulsive interactions increase the spectral weight in the subband with the largest charge velocity, leading

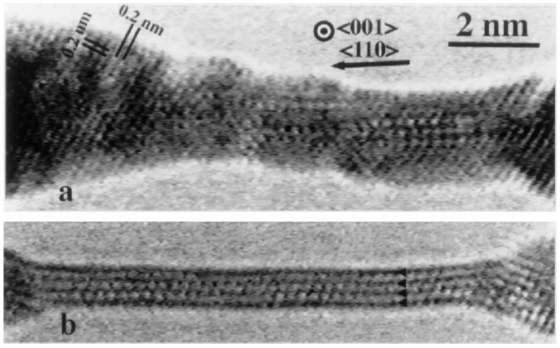

Figure 1. Transmission electron micrographs showing the formation of a gold nanowire, from Ref. [12]: (**a**) an image of Au(001) film with closely spaced nanoholes, the initial stage of the nanowire; (**b**) a nanowire four atoms in diameter, resulting from further electron-beam irradiation.

to an enhancement of the persistent current induced by an Aharanov-Bohm flux threading the ring at low temperatures [1, 2].

Wang also supervised the master's thesis of Jérôme Bürki at the École Polytechnique Fédérale de Lausanne, and recommended Jérôme to Dionys Baeriswyl, Xenophon Zotos, and myself as a doctoral student to work on a project on metallic nanocohesion funded by the Swiss National Foundation. This was very serendipitous, since that project [3]–[7] was ultimately recognized by the Swiss Physical Society with their 2000 ABB Prize, shared by Dr. Bürki and myself. And this work certainly played no small part in my securing a tenure-track position at the University of Arizona.

I thus think it appropriate, in this volume in honor of Deng Feng Wang, to discuss my most recent work [8] on metallic nanowires. Motivated by Wang's love of mathematical rigor, I will present some of the mathematical details of our stability calculation, which have not been previously published.

2. The remarkable stability of the thinnest metal wires

In the past eight years, experimental research on atomically-thin metal wires has burgeoned [9]–[18]. Perhaps the most remarkable feature of metal nanowires is the fact that they are stable at all. Fig. 1 shows electron micrographs illustrating the formation of a gold nanowire [12]. Under electron beam irradiation, the wire becomes ever thinner, until it is but four atoms in diameter. Almost all of the atoms are at the

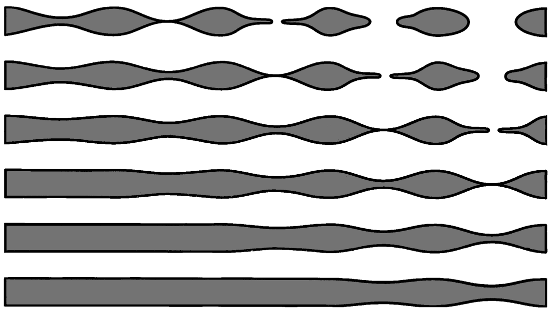

Figure 2. Artist's conception of a propagating Rayleigh instability, from Ref. [21].

surface, with reduced coordination numbers. The surface energy of such a structure is enormous, yet it is observed to form spontaneously, and to persist almost indefinitely. Even wires one atom thick are found to be stable for days at a time [14, 15].

A cylindrical body longer than its circumference is unstable to breakup under surface tension [19, 20], a phenomenon known as the *Rayleigh instability* (see Fig. 2). How then to explain the durability of long gold nanowires [c.f. Fig. 1(b)], the thinnest of which have been shown [18] to be almost perfectly cylindrical in shape? The key is the quantum corrections [8] to the classical stability coefficients.

Only axially-symmetric deformations can lower the surface energy of a cylindrical object, and thus lead to an instability [20]. Any such deformation may be written as a Fourier series

$$R(z) = R_0 + \int_{-\infty}^{\infty} dq\, b(q) e^{iqz}, \tag{1}$$

where $R(z)$ is the radius of the cylinder at z, R_0 is the unperturbed radius, and $b(q)$ is a complex perturbation coefficient. When the wire deforms, the atoms rearrange themselves, but the volume per atom remains essentially constant [6, 22]. The constant-volume constraint leads to the condition

$$b(0) = -\frac{1}{R_0} \int_{0}^{\infty} dq\, |b(q)|^2. \tag{2}$$

Other physically reasonable constraints are also possible [6], but lead to similar results. Thus the problem is to determine the energetics of a nanowire as a functional of the Fourier coefficients $b(q)$.

3. Free electron model

We investigate the simplest possible model [3, 22] for a metal nanowire: a free (conduction) electron gas confined within the wire by Dirichlet boundary conditions. A nanowire is an open system, connected to macroscopic metallic electrodes at each end [9]–[18]. Therefore the change of the grand canonical potential Ω under the perturbation determines its stability. Ω is related to the electronic density of states (DOS) $g(E)$ by

$$\Omega = -\frac{1}{\beta} \int dE\, g(E) \ln\left(1 + e^{-\beta(E-\mu)}\right), \tag{3}$$

where β is the inverse temperature and μ is the electrochemical potential of electrons injected into the nanowire from the macroscopic electrodes. The DOS of an open system may be expressed in terms of the scattering matrix as [23]

$$g(E) = \frac{1}{2\pi i} \mathrm{Tr} \left\{ S^{\dagger}(E) \frac{\partial S}{\partial E} - \mathrm{H.c.} \right\}. \tag{4}$$

This formula is also known as the *Wigner delay*. Note that in Eq. (4), a factor of 2 for spin degeneracy has been included.

Our aim is to expand Ω up to second order in the coefficients $b(q)$ characterizing the deformation. As we will show, this yields

$$\Omega[b] = \Omega[0] + \int_0^{\infty} dq\, \alpha(q) |b(q)|^2 + \mathcal{O}(b^3), \tag{5}$$

where the stability coefficient $\alpha(q)$ depends implicitly on R_0 and temperature. The change in the grand canonical potential is of second order in b and contributions from deformations with different q decouple. If $\alpha(q)$ is negative for any value of q, then Ω decreases under the deformation and the wire is unstable.

For a translationally-invariant wire, the transverse motion is quantized, leading to the formation of discrete electronic subbands [1, 2]. The total DOS is the sum of the contributions from each subband (see Fig. 3): every subband begins to contribute at a threshold energy equal to the energy of its quantized transverse motion with a sharp spike, falling off smoothly for increasing energy. If the Fermi energy ε_F lies near one of these sharp peaks, certain small deformations of the wire can dramatically increase the DOS. According to (3), this lowers the grand canonical potential, leading to an instability. On the other hand, if there is no subband threshold sufficiently close to ε_F, we find that the DOS instead decreases with any deformation, implying the existence of stable regions in the intervals between the instabilities associated with the opening of each subband.

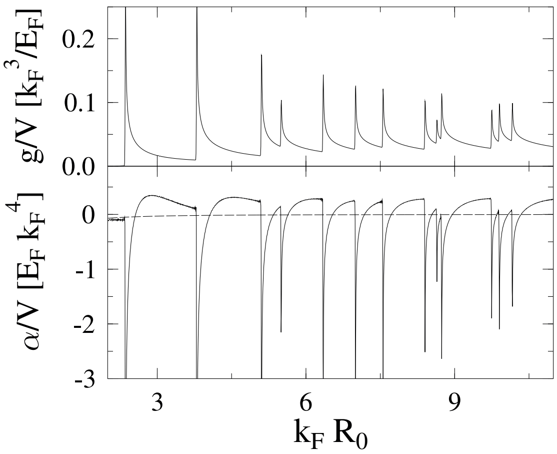

Figure 3. Density of states $g(\varepsilon_F)$ of a cylindrical wire (upper diagram) and stability coefficient α at zero temperature (lower diagram) versus the radius R_0 of the unperturbed wire. The wavevector of the perturbation is $qR_0 = 1$. Dashed curve: Weyl contribution to α.

4. Weyl expansion

To examine this picture quantitatively, it is useful to perform a systematic semiclassical expansion [24, 25] of the DOS, $g(E) = \bar{g}(E) + \delta g(E)$, where $\bar{g}$ is a smooth average term, referred to as the Weyl contribution, and $\delta g(E)$ is an oscillatory term, whose average is zero. For the free electron model with Dirichlet boundary conditions, the Weyl term is [25]

$$\bar{g}(E) = E^{-1}\left(\frac{k_E^3 V}{2\pi^2} - \frac{k_E^2 A}{8\pi} + \frac{k_E K}{6\pi^2}\right), \tag{6}$$

where $k_E = \sqrt{2mE}/\hbar$, V is the volume of the wire, A its surface area, and K the integrated mean curvature of its surface. Inserting Eq. (6) into Eq. (3), one finds the following semiclassical expansion at zero temperature:

$$\frac{\Omega}{\varepsilon_F} = -\frac{2k_F^3 V}{15\pi^2} + \frac{k_F^2 A}{16\pi} - \frac{2k_F K}{9\pi^2} + \frac{\delta\Omega}{\varepsilon_F}. \tag{7}$$

One can show [6] that interaction effects are higher order in $\hbar$.

The energy cost of the deformation can be calculated in the Weyl approximation by simple geometrical considerations, and is

$$\begin{aligned}\Delta\bar{\Omega}/\varepsilon_F &= \left(-\frac{8}{15}k_F^3 R_0 + \frac{\pi}{4}k_F^2\right) b(0) \\ &\quad + \int_0^\infty dq \left[-\frac{8k_F^3}{15} + \left(\frac{\pi k_F^2 R_0}{4} - \frac{8k_F}{9}\right) q^2\right] |b(q)|^2. \qquad (8)\end{aligned}$$

The constraint (2) can be used to eliminate $b(0)$ in Eq. (8), so that $\Delta\bar{\Omega}$ is quadratic in b, as expected.

5. Trace formulas

The oscillatory contribution $\delta g(E)$ to the DOS may be approximated as a Feynman sum over classical periodic orbits à la Gutzwiller [24, 25]. Since we are interested in modeling nanowires which possess axial and/or translational symmetries, we can not utilize Gutzwiller's original trace formula [26], which describes systems whose periodic orbits are isolated, but must instead employ a generalization due to Creagh and Littlejohn, describing a system with an f-dimensional Abelian symmetry [27]:

$$\delta g(E) = \frac{2}{\pi\hbar}\frac{1}{(2\pi\hbar)^{f/2}}\sum_\Gamma \frac{T_\Gamma V_\Gamma J_\Gamma^{-1/2}}{|\det \tilde{M}_\Gamma - 1|^{1/2}} \cos\left(\frac{S_\Gamma}{\hbar} - \frac{\sigma_\Gamma \pi}{2} - \frac{f\pi}{4}\right), \quad (9)$$

where the sum runs over f-dimensional families Γ of degenerate periodic orbits, T_Γ is the period of an orbit in Γ, V_Γ is the f-dimensional volume spanned by Γ, S_Γ is the action of the orbit, and σ_Γ is a phase shift determined by the singular points along the classical trajectory. The quantity $\tilde{M}$ is the so-called monodromy matrix, characterizing the stability of the orbit with respect to perturbations. It describes as a Poincaré map the linearized motion of small perturbations from the periodic orbit in a surface of section perpendicular to the orbit in phase space: an initial variation of momentum and position in the surface of section $(\delta r, \delta p)$ is related to the mismatch $(\delta r', \delta p')$ after one period by

$$\begin{pmatrix} \delta r' \\ \delta p' \end{pmatrix} = \tilde{M} \begin{pmatrix} \delta r \\ \delta p \end{pmatrix}. \qquad (10)$$

Finally, the factor $J_\Gamma = |\det(\partial r'/\partial p)|$.

We shall also need to consider the breaking of continuous symmetries, which is elegantly described in terms of semiclassical perturbation theory [28, 29], wherein the cosine in the trace formula is replaced by

$$\cos(S_\Gamma/\hbar + \theta_\Gamma) \to \mathrm{Re}\left\{e^{i(S_\Gamma/\hbar + \theta_\Gamma)} \left\langle e^{i\Delta S_\Gamma/\hbar}\right\rangle_\Gamma\right\}, \qquad (11)$$

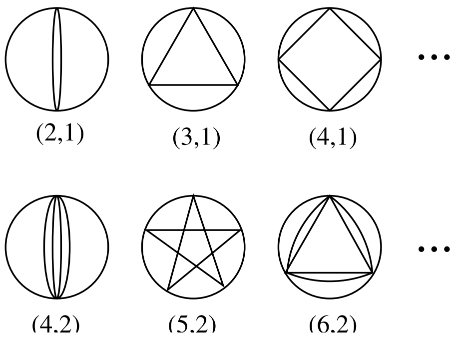

Figure 4. Periodic orbits of an electron in a cross-section of the wire, labeled (v, w), where v is the number of vertices and w the winding number. The length of an orbit is $L_{vw} = vD^* \sin\phi_{vw}$, where $\phi_{vw} = \pi w/v$ is the angle of incidence at a vertex.

where

$$\langle e^{i\Delta S_\Gamma/\hbar}\rangle_\Gamma = V_\Gamma^{-1} \int d\mu(g) e^{i\Delta S_\Gamma(g)/\hbar} \tag{12}$$

is an average over the measure of the broken symmetry group.

For an axially-symmetric three-dimensional nanowire, the periodic orbits (see Fig. 4) occur in one-dimensional families which fit within the circular cross-section of the wire. For the unperturbed cylinder, Eq. (9) yields

$$\delta g(E) = \frac{mL}{\pi\hbar^2} \sum_{w=1}^{\infty} \sum_{v=2w}^{\infty} \frac{f_{vw} L_{vw}}{v^2} \cos(k_E L_{vw} - 3v\pi/2), \tag{13}$$

where $f_{vw} = 1 + \theta(v - 2w)$ counts the discrete symmetry of the orbit under time-reversal and the remaining terms are defined in the caption of Fig. 4. The DOS given by the sum of Eqs. (6) and (13) is plotted in the upper part of Fig. 3.

The deformation (1) breaks the translational symmetry of the wire. The corresponding modulation factor (12) arising in semiclassical perturbation theory is

$$\langle e^{i\Delta S_{vw}(z)/\hbar}\rangle_z = \frac{1}{LR_0} \int_0^L dz\, R(z)\, e^{i\Delta S_{vw}(z)/\hbar}, \tag{14}$$

where

$$\frac{\Delta S_{vw}(z)}{\hbar} = 2v \sin\phi_{vw} k_E \int_{-\infty}^{\infty} dq\, b(q) e^{iqz}. \tag{15}$$

Expanding δg up to second order in $b(q)$ gives

$$\Delta\{\delta g(E)\} = \frac{4m}{\hbar^2}\sum_{w=1}^{\infty}\sum_{v=2w}^{\infty}\frac{f_{vw}\sin\phi_{vw}}{v}\left[b(0)(\cos\theta_{vw} - k_E L_{vw}\sin\theta_{vw})\right.$$
$$\left. - \frac{k_E L_{vw}}{R_0}\int_0^{\infty} dq\,|b(q)|^2\left(\sin\theta_{vw} + \frac{k_E L_{vw}}{2}\cos\theta_{vw}\right)\right], \quad (16)$$

where $\theta_{vw}(E) = k_E L_{vw} - 3v\pi/2$. The constraint (2) can be used to eliminate $b(0)$ in Eq. (16), so that $\Delta\{\delta g(E)\}$ is also quadratic in b.

6. Stability analysis

Inserting Eq. (16) into Eq. (3), and performing the energy integral, one obtains the oscillatory quantum correction $\delta\Omega$ up to quadratic order in the Fourier coefficients $b(q)$ of the perturbation. Combining $\delta\Omega$ so determined with Eq. (8) yields Eq. (5), as advertised.

Let us first discuss the stability of a nanowire at zero temperature. Fig. 3 shows the stability coefficient and DOS at the classical stability threshold $qR_0 = 1$ as a function of R_0. The quantum correction destabilizes the wire where the DOS is sharply peaked; but what is more surprising, it *stabilizes* the wire in the intervening intervals.

With these results, we can construct the zero temperature stability diagram for the wire (see Fig. 5(a)). In contrast to Plateau's classical stability analysis [19], an additional quantum length scale arises here, namely the Fermi wavelength λ_F. The stability problem is now determined by two dimensionless parameters: qR_0 and $k_F R_0$. In Fig. 5, regions of instability, where $\alpha(q) < 0$, are shaded grey, while stable regions are shown in white. Note that many of the white regions of stability persist all the way down to $q = 0$, indicating that an infinitely long wire is a true metastable state if its radius lies in one of the windows of stability. The *multistability* of the system, indicated by the alternating stable and unstable stripes, reflects commensurability effects between λ_F and R_0.

The electrical conductance G of a perfect cylindrical nanowire is quantized [30] in units of $G_0 = 2e^2/h$. The quantized conductance values of the stable cylindrical configurations are indicated by bold numerals in Fig. 5(a). For comparison, the right vertical axis of the figure is labeled with the corrected Sharvin conductance [30]

$$G_S = \left(\frac{k_F R_0}{2}\right)^2\left(1 - \frac{2}{k_F R_0}\right), \quad (17)$$

which gives a smooth approximation to G/G_0. The conductance values of the stable configurations are somewhat analogous to the *magic numbers* of enhanced stability in atomic nuclei [25] and metal clusters

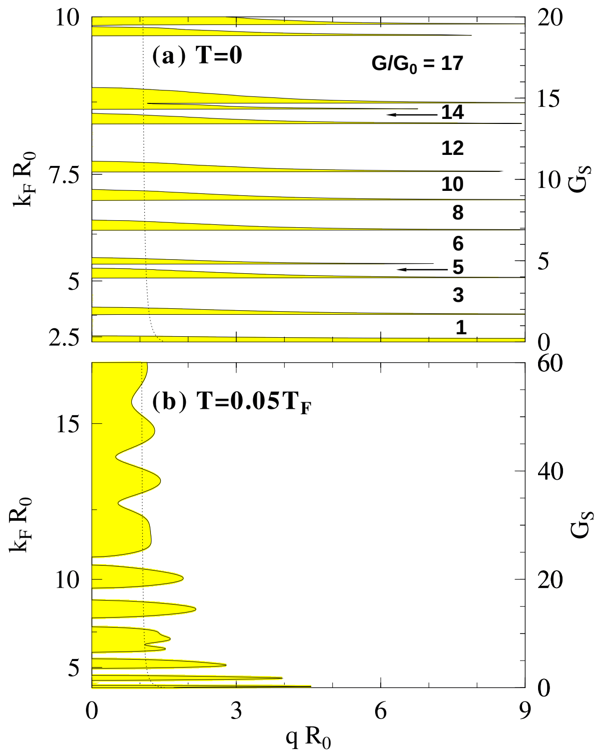

Figure 5. Stability diagram for cylindrical nanowires at two different temperatures. White areas are stable, grey unstable to small perturbations. The quantized electrical conductance values G of the stable configurations are indicated by bold numerals in (**a**), with $G_0 = 2e^2/h$. Right vertical axis: corrected Sharvin conductance G_S. Dotted curve: stability criterion in the Weyl approximation.

[25, 31]. An important distinction is that the magic numbers in nuclei and clusters refer to the number of fermions in a finite system, while we consider an infinite, open system, with magic numbers describing the number of conducting transverse modes [3] which hold the wire together (the number of conducting modes is approximately equal to the number of atoms which fit within a cross section of the wire). The sequence of magic numbers $G/G_0 = 1, 3, 5, 6, \ldots$ is consistent with the observation of conductance quantizaton in alkali metal nanowires [10, 16, 17].

7. Classical Limit

At zero temperature, the pattern of stable regions separated by unstable stripes shown in Fig. 5(a) continues up to arbitrarilly large radii. However, at any finite temperature T, the quantum oscillations in α are smoothed out, and the classical stability criterion $qR_0 > 1$ is recovered asymptotically for sufficiently large radii. The crossover from the $T = 0$ result to the classical limit occurs when $k_BT \sim E_F(G_0/G)$, i.e., when the thermal energy k_BT is comparable to the average transverse level spacing. Fig. 5(b) shows the stability diagram for $T/T_F = .05$, where $T_F = E_F/k_B$ is the Fermi temperature. One sees that the stability boundary indeed begins to cross over to the classical line $qR_0 = 1$ for $G_S > 20$.

In Fig. 5(b), there are no true metastable configurations with $G_S > 25 \sim T_F/T$, indicating that all thicker wires would be dynamically unstable (like a column of fluid) at this temperature, once the electronic shell effects have been smoothed out. However, $T_F = 3.75 \times 10^4$K in sodium, so multistability from electronic shell effects can be expected to occur in sodium contacts [16, 17] with $G/G_0 \leq 125$ up to at least 300K.

It should be pointed out that thermal averaging is not the only mechanism which can suppress electronic shell effects. Disorder also tends to smooth out the sharply peaked structure in the density of states, so that one can expect a reduction of shell effects when the diameter of the wire exceeds the mean free path. Furthermore, the tendency of the positive ions to order themselves into regular arrays [12, 18] will certainly affect the stability of metallic nanowires. Indeed, pioneering theoretical investigations [32, 33, 34] of the dynamics of nanowires focused exclusively on the arrangement of the ions. Based on the relative importance of electronic shells and crystal structure in metal clusters [31], one would expect electronic shell effects to dominate the energetics of very thin wires, particularly in the alkali metals, with crystal structure becoming increasingly important for thicker wires, and for metals where the bonding is more directional.

8. Conclusions

We have shown that the subband structure [1, 2] of a metal nanowire has a profound effect on its mechanical stability. Our finding that the instability of an atomically-thin metal wire under surface tension can be completely suppressed by quantum-size effects is likely to be important to the eventual commercial development of nanoscale integrated circuits, since it suggests that stable metal interconnects one atom wide are possible. Indeed, linear chains composed of four to seven gold atoms suspended between two gold electrodes, with a conductance $G = G_0$, were found to be stable in the laboratory for hours at a time [14, 15]. Given that such a configuration has an enormous surface energy, its stability is at first sight surprising. However, in our free electron model, we find that an infinitely long wire with a conductance of G_0 is indeed stable with respect to small perturbations.

Finally, let us comment on the dynamical evolution of a nanowire under elongation or compression. Consider stretching a nanowire that is initially in a stable configuration (white areas in Fig. 5). Under elongation, the radius of the wire decreases, so that one moves downward on the stability diagram. When a stability boundary is encountered, it becomes energetically (and dynamically) favorable for the wire to deform spontaneously, until another stable configuration of smaller radius is reached, thus causing the conductance to jump abruptly from one magic number to a smaller one, and conversely under compression. This scenario is consistent with the claim [11] that the structure of a metallic nanowire undergoes a sequence of abrupt changes as a function of elongation or compression. The finite widths of the unstable tongues in Fig. 5 also provides a possible explanation for the hysteresis [11] observed in the conductance as a function of elongation: the critical radius at which the wire's conductance jumps between neighboring magic numbers is different, depending on whether the tongue is approached from above or below, i.e., depending on whether the wire is stretched or compressed.

Acknowledgments

I wish to thank Raymond Goldstein, Hermann Grabert, and especially Frank Kassubek, without whose efforts and insights this work would not have been possible. I also want to thank Helen Giesel for sharing the endless Summer in Arizona with me. This research was supported by NSF Grant DMR0072703 and by an award from Research Corporation.

References

[1] C. A. Stafford and D. F. Wang, Z. Phys. B 103, 323 (1997).

[2] C. A. Stafford and D. F. Wang, Phys. Rev. B 56, R4383 (1997).

[3] C. A. Stafford, D. Baeriswyl, and J. Bürki, Phys. Rev. Lett. **79**, 2863 (1997).

[4] J. Bürki, C. A. Stafford, X. Zotos, and D. Baeriswyl, Phys. Rev. B **60**, 5000 (1999).

[5] J. Bürki and C. A. Stafford, Phys. Rev. Lett. 83, 3342 (1999).

[6] C. A. Stafford, F. Kassubek, J. Bürki, and H. Grabert, Phys. Rev. Lett. **83**, 4836 (1999).

[7] C. A. Stafford, J. Bürki, and D. Baeriswyl, Phys. Rev. Lett. 84, 2548 (2000).

[8] F. Kassubek, C. A. Stafford, H. Grabert, and R. E. Goldstein, Nonlinearity **14**, 167 (2001).

[9] For a review, see *Nanowires*, P. A. Serena and N. Garcia eds. (Kluwer Academic, Dordrecht, 1997).

[10] J. M. Krans, J. M. van Ruitenbeek, V. V. Fisun, I. K. Yanson, and L. J. de Jongh, Nature **375**, 767 (1995).

[11] G. Rubio, N. Agraït, and S. Vieira, Phys. Rev. Lett. **76**, 2302 (1996).

[12] Y. Kondo and K. Takayanagi, Phys. Rev. Lett. **79**, 3455 (1997).

[13] J. L. Costa-Krämer *et al.,* PRB **55**, 5416 (1997).

[14] H. Ohnishi, Y. Kondo, and K. Takayanagi, Nature **395**, 780 (1999).

[15] A. I. Yanson *et al.*, Nature **395**, 783 (1999).

[16] A. I. Yanson, I. K. Yanson, and J. M. van Ruitenbeek, Nature **400**, 144 (1999).

[17] A. I. Yanson, I. K. Yanson, and J. M. van Ruitenbeek, Phys. Rev. Lett. **84**, 5832 (2000).

[18] Y. Kondo and K. Takayanagi, Science **289**, 606 (2000).

[19] J. Plateau, *Statique experimentale et theorique des liquides soumis aux seules forces moleculaires*, (Gautier-Villars, Paris, 1873).

[20] S. Chandrasekhar, *Hydrodynamic and Hydromagnetic Stability* (Dover, New York, 1981) pp 515-74.

[21] T. R. Powers and R. E. Goldstein, Phys. Rev. Lett. **78**, 2555 (1997).

[22] F. Kassubek, C. A. Stafford, and H. Grabert, Phys. Rev. B **59**, 7560 (1999).

[23] R. Dashen, S.-K. Ma, and H. J. Bernstein, Phys. Rev. **187**, 345 (1969).

[24] M. C. Gutzwiller, *Chaos in Classical and Quantum Mechanics* (Springer, New York, 1990).

[25] M. Brack and R. K. Bhaduri, *Semiclassical Physics.* (Addison-Wesley, Reading, MA, 1997).

[26] M. C. Gutzwiller, J. Math. Phys. **12**, 343 (1971).

[27] S. C. Creagh and R. G. Littlejohn, Phys. Rev. A **44**, 836 (1991).

[28] D. Ulmo, M. Grinberg, and S. Tomsovic, Phys. Rev. E **54**, 136 (1996).

[29] S. C. Creagh, Ann. Phys. (N.Y.) **248**, 60 (1996).

[30] J. A. Torres, J. I. Pascual, and J. J. Sáenz, Phys. Rev. B **49**, 16581 (1994).

[31] W. A. de Heer, Rev. Mod. Phys. **65**, 611 (1993).

[32] U. Landman et al., Science **248**, 454 (1990).

[33] T. N. Todorov and A. P. Sutton Phys. Rev. Lett. **70**, 2138 (1993).

[34] M. R. Sørensen, M. Brandbyge, and K. W. Jacobsen, Phys. Rev. B **57**, 3283 (1998).